Using graph theory to analyze the vulnerability of process plants in the context of cascading effects

Reference:

Khakzad Nima, Reniers Genserik.- Using graph theory to analyze the vulnerability of process plants in the context of cascading effects

Reliability engineering and system safety - ISSN 0951-8320 - 143(2015), p. 63-73

DOI: http://dx.doi.org/doi:10.1016/j.ress.2015.04.015

Handle: http://hdl.handle.net/10067/1273350151162165141

Using graph theory to analyze the vulnerability of process plants in the context of cascading effects

Nima Khakzad[a], Genserik Reniers[b,c,d]

a. Safety and Risk Engineering Group (SREG), Memorial University of Newfoundland, St. John's, NL, Canada A1B 3X5

Email: nkhakzad@gmail.com

Phone: +1 709 769 2345

b. TU Delft, Faculty of Technology, Policy and Management, Safety and Security Science Group (S.3G), 2628 BX Delft, The Netherlands

c. Universiteit Antwerpen, Faculty of Applied Economics, Antwerp Research Group on Safety and Security (ARGoSS), 2000 Antwerp, Belgium

d. KULeuven, Campus Brussels, Research Group CEDON, 1000 Brussels, Belgium

Email: G.L.L.M.E.Reniers@tudelft.nl

Phone: +31 15 27 83749

Abstract

Dealing with large quantities of inflammable and explosive materials, usually at high-pressure high-temperature conditions, makes process plants very vulnerable to cascading effects compared with other infrastructures. The combination of the extremely low frequency of cascading effects and the high complexity and interdependencies of process plants makes risk assessment and vulnerability analysis of process plants very challenging in the context of such events. In the present study, cascading effects were represented as a directed graph; accordingly, the efficacy of a set of graph metrics and measurements was examined in both unit and plant-wide vulnerability analysis of process plants. We demonstrated that vertex-level closeness and betweenness can be used in the unit vulnerability analysis of process plants for the identification of critical units within a process plant. Furthermore, the graph-level closeness metric can be used in the plant-wide vulnerability analysis for the identification of the most vulnerable plant layout with respect to the escalation of cascading effects. Furthermore, the results from the application of the graph metrics have been verified using a Bayesian network methodology.

Keywords: Cascading effect; Process plant; Vulnerability analysis; Graph metrics; Bayesian network.

1. Introduction

Process plants are normally characterized by a number of dependent and interlinked components which contain, carry, or process hazardous (e.g., inflammable, explosive, toxic) materials usually in high-temperature high-pressure conditions. As a result, an otherwise ordinary accident or undesired event which could be tolerated or controlled in other industrial plants has the potential of turning into a catastrophe within a few hours due to the possibility of triggering a cascading effect. Cascading effects (also known as domino effects or chains of accidents) in the process industry are low-frequency high-consequence chains of accidents. In case of a cascading effect, a primary accident (e.g., a fire) in a primary unit (e.g., a storage tank) propagates to neighboring units and triggers secondary accidents in the vicinity of the primary unit and so forth. To consider it a cascading effect, the overall consequences of such a sequence of accidents should be higher than those of the primary event [1]. Usually, the final outcome of a cascading effect is several orders of magnitude more severe than that of the primary accident.

The propagation of the primary accident is usually carried out by means of escalation vectors such as fire impingement, fire engulfment or heat radiation in the case of fires, and overpressure wave or projectile fragments in the case of explosions. These escalation vectors help the primary accident to propagate by causing damage (loss of containment or loss of physical integrity) to adjacent units (target units). The probability of escalation, however, depends on a variety of factors such as the type of the primary accident and the intensity of escalation vectors, the distance between the primary unit and the target units, the vulnerability of the target units, and the type and inventory of chemical substances involved [2].

In spite of their extremely low frequency, the possibility of cascading effects should not be ignored in safety risk assessment and vulnerability analysis of process plants. In fact, high complexity and interdependencies within process plants make them increasingly vulnerable to cascading effects. For instance, LPG[1]-induced cascading effects in Mexico City in November 1984 left 650 deaths and 6500 injuries and destructed three process plants. Most recently, in December 2005, a series of fires and explosions in an oil storage plant in the Buncefield Complex, in the United Kingdom, led to the largest fire in peacetime Europe, leaving 43 injuries and causing huge devastation in the area [3]. Cascading effects have long been recognized in process plants and chemical infrastructures [4-7], and have been studied in risk assessment and management of process plants over the past decade [8-21].

In the context of safety risk assessment and management of critical infrastructures, however, other factors such as vulnerability, robustness, and resilience should also be taken into account [16,22,23]. Johansson et al. [23] use the term vulnerability "as the inability of a system to withstand strains and the effects of failures". In the present study, however, vulnerability is defined as the capability of a process plant to foster either the onset or the escalation of potential cascading effects. On the contrary, robustness can be defined as the ability of the process plant to hamper the escalation of cascading effects. As a result, vulnerability and robustness can be regarded as two complementary terms in this context. While the aim of traditional risk analysis is to identify hazardous events, their likelihood and potential consequences, the aim of vulnerability analysis is to explore the system weaknesses by identifying those critical components whose failure can adversely affect the performance of the system. Compared with risk analysis, in

[1]Liquefied Petroleum Gas

vulnerability analysis, however, the failure probabilities are less important and more emphasis is given to the extent and severity of the consequences [24]. Furthermore, vulnerability analysis is usually performed using deterministic or analytical techniques – as opposed to probabilistic methods used in risk analysis – to seek the impact of accidental or intentional failures on the performance of a system [16,22].

Vulnerability analysis can be considered from two perspectives: (i) plant vulnerability and (ii) unit vulnerability. Plant vulnerability can be interpreted as an inherent characteristic of a process plant to measure how far and to what extent the adverse effects of a primary accident can propagate through the plant. This interpretation of vulnerability can be beneficial when deciding among alternative layouts in the early design stage of process plants so that the most robust layout could be selected. Unit vulnerability analysis, however, can be carried out to identify critical units within a process plant. This interpretation of vulnerability can be employed to allocate proactive countermeasures to the weak points and critical units so that the onset of cascading effects can be prevented or their escalation can be hampered. Generally speaking, in a chain of accidents which starts from unit A, traverses unit B, and terminates at unit C (i.e., $A \rightarrow B \rightarrow C$), A, B, and C are known as source, intermediate, and sink or terminal units, respectively [16]. In a process plant, a critical component can be deemed as either (i) a source unit whose failure would cause large adverse consequences to the plant (critical initiating unit) or (ii) an intermediate unit whose failure helps escalate a previously occurred accident through the plant to a large extent (critical transmitting unit) or (iii) a unit which turn outs to be the sink unit in many potential cascading effects with different sequences of source and intermediate units within a process plant (critical terminal unit).

Compared to well-established methods available in risk analysis of cascading effects, relevant work in the field of vulnerability analysis has been very few [16,20,21,25-27]. Cozzani et al. [25] introduced a set of domino indices to score and identify critical units within process plants with respect to escalation events. Khakzad et al. [20] established a Bayesian network methodology to identify the most probable sequence of accidents (i.e., $\max_{A,B,C} P(A \rightarrow B \rightarrow C)$) in a process plant. Most recently, Reniers and Audenaert [16] used a network theory to rank most vulnerable intermediate and terminal units based on "terminal and propagation vulnerability indices". Similar work has been conducted to determine safety distances and safety inventories [21,26] in

order to reduce the vulnerability of process plants subject to cascading effects. Representing a process plant by means of nodes (units of the plant) and edges (escalation vectors among the units) of a graph in this study, we aim to explore the applicability and efficiency of a set of graph metrics to both unit and plant vulnerability analysis of process plants, and chemical infrastructures in general, in the context of cascading effects.

This paper is organized as follows. The basic concepts and escalation mechanism of cascading effects within process plants are recapitulated in Section 2. The graph theory metrics used in this work are introduced and briefly explained in Section 3. A brief description of Bayesian networks and its application to modeling cascading effects [20] is replicated in Section 4. In Section 5, we apply graph metrics to vulnerability analysis of hypothetical process plants in order to identify most critical initiating and transmitting units within a plant (unit vulnerability analysis) and also to rank different plant layouts in terms of vulnerability (plant vulnerability analysis), and then compare the results obtained from the application of graph metrics with those from the Bayesian network methodology. The main conclusions drawn from this work have been presented in Section 6.

2. Terminology and escalation mechanism of cascading effects

Cascading effects take place when an accident in a unit (primary unit) propagates to other units (secondary units) by means of escalation vectors. Escalation vectors are physical effects such as fire impingement, fire engulfment, or heat radiation in the case of a fire, and deflagration overpressure or projectile fragments in the case of an explosion. Simple methods for calculation of escalation vectors can be found in [28-30]. The probability of escalation, however, depends not only on the type and intensity of escalation vectors but also on the inventory of chemicals and the vulnerability of target units. Moreover, to determine if a target unit is likely to be impacted by an escalation vector, the intensity of the escalation vector at the point of interest (i.e., the location of the target unit) should be higher than a corresponding threshold value[2]. For example, for atmospheric vessels (e.g., atmospheric storage tanks) the threshold values for the heat radiation and the overpressure have been proposed as $Q_{th} = 15\ \frac{kw}{m^2}$ and $P_{th} = 22\ kpa$, respectively [25].

[2] If the intensity of the escalation vector is below a threshold value, the likelihood of escalation would be practically negligible.

Figure 1 shows the onset of a cascading effect in which a fire (primary accident) in the unit X1 (primary unit) is likely to impact the neighboring units X2 and X3 but not X4. The reason is the intensity of the escalation vectors (here heat radiation) received by X2 (Q_{12}) and X3 (Q_{13}) is above the threshold value (i.e.,$Q_{12} = Q_{13} = 20\frac{kW}{m^2} > Q_{th} = 15\ \frac{kW}{m^2}$), while that of X4 ($Q_{14}$) is not (i.e., $Q_{14} = 8\ \frac{kW}{m^2} < Q_{th} = 15\ \frac{kW}{m^2}$). Therefore, X2 and X3 could be selected as potential secondary units involved in the cascading effect, helping to escalate the cascading effect to the first level[3]. After either X2 or X3 is involved in the cascading effect, it can contribute with X1 to impact X4 to escalate the cascading effect to the second level only if the superposition of the respective escalation vectors is greater than the corresponding threshold value, which is the case for the cascading effect shown in Figure 1 (i.e., $Q_{14} + Q_{24} + Q_{34} = 28\frac{kW}{m^2} > Q_{th} = 15\frac{kW}{m^2}$). This contribution of units (the primary and secondary units) to impact another unit (tertiary unit) is known as the synergistic effect [20,21].

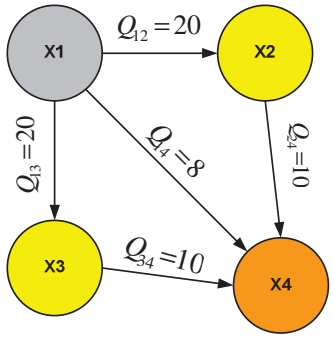

Figure 1. Propagation of a cascading effect. The primary X1 and secondary units X2 and X3 cooperate to impact the tertiary unit X4 through synergistic effect. The intensity of heat radiation emitted by unit "i" and received by unit "j"is denoted by Q_{ij} on each edge.

Among methods available to estimate the escalation probabilities, probit models [8-10] have been very popular due to their simplicity and flexibility which facilitate their application to a wide variety of accident scenarios, escalation vectors, and target units with different vulnerabilities. Using probit models, usually both the type of a unit (e.g., atmospheric or

[3] The primary accident in X1 is considered as a zero-level cascading effect since a chain of accidents has not yet formed.

pressurized) and the type of escalation vector the unit receives (e.g., heat radiation or overpressure) are taken into consideration to calculate a probit value Y in the form of:

$$Y = a + b.\ln(D) \quad (1)$$

where a and b represent probit coefficients determined using experimental data and regression methods; D is either the escalation vector (e.g., heat radiation intensity) or relevant parameters such as ttf of the secondary unit. Table 1 presents some probit models for vulnerability analysis of atmospheric and pressurized units exposed to heat radiation and overpressure [9]. In Table 1, Y is probit value; ttf is the time to failure of the secondary unit in (s); Q is the received heat radiation in (kW/m^2); V is the volume of the secondary unit in (m^3).

Table 1.Probit models for heat radiation [9]

Type of unit	Escalation vector	Probit model
Atmospheric	Heat radiation	$Y = 12.54 - 1.847 \ln(ttf)$ $\ln(ttf) = -1.13 \ln(Q) - 2.67 \times 10^{-5}V + 9.9$
Pressurized	Heat radiation	$Y = 12.54 - 1.847 \ln(ttf)$ $\ln(ttf) = -0.95 \ln(Q) + 8.85V^{0.032}$

Having Y determined (e.g., by using the probit models given in Table 1), the escalation probability could be estimated as:

$$P = \phi\,(Y - 5) \quad (2)$$

where ϕ is the cumulative density function of the standard normal distribution. For spreadsheet applications, however, the escalation probability can alternatively be approximated from the following relationship:

$$P = 50\left\{1 + \frac{Y-5}{|Y-5|}\,\mathrm{erf}\left(\frac{|Y-5|}{\sqrt{2}}\right)\right\} \quad (3)$$

where erf is the error function.

3. Graph theory: metrics and measurements

A mathematical graph is an ordered pair $G = (V, E)$ comprising a set of vertices $V = \{v_1, v_2, \dots, v_n\}$ and a set of edges $E = \{e_1, e_2, \dots, e_m\}$. The order of a graph is determined by the number of its vertices $|V| = n$ while the size of a graph is the number of its edges $|E| = m$. A vertex can simply be represented as a node, and an edge can be drawn as a line, directed or undirected, connecting two vertices. In a weighted graph, a set of numerical values can also be

assigned to either the vertices or edges of the graph. In this case, the weighted graph can be presented as $G = (V, E, w_V, w_E)$ in which w_V and w_E are weight vectors allocated to vertices and edges, respectively.

In a directed graph, a walk from the vertex v_i to v_j is a sequence of vertices and edges starting from v_i and ending in v_j when each intermediate vertex can be traversed several times. A path, however, is a walk from v_i to v_j where each intermediate vertex is traversed only once. Similarly, the geodesic distance betweenv_i and v_j, denoted by $d_{ij} = d(v_i, v_j)$, is the length of the shortest path from v_i to v_j. If there is no path between v_i and v_j, then $d_{ij} = \infty$. A path that starts and ends at the same vertex is called a cycle, and a graph that contains at least a cycle is called cyclic. Otherwise, the graph is acyclic.

In graph theory, there have been developed metrics and indices either to identify most important (critical) vertices or to rank different graph structures. Accordingly, the relevant metrics in this work are divided into two categories: (i) vertex-level metrics and (ii) graph-level metrics. The former category is used to identify and rank critical vertices within a graph (i.e., unit vulnerability analysis) while the latter category is used to compare different graph structures based on their vulnerability (i.e., plant vulnerability analysis). We briefly describe each category in the following sections.

3.1.Vertex metrics

A variety of metrics have been proposed for graph vertices among which 'degree', 'betweenness', and 'closeness' measures [31] have been very popular. The degree of a vertex v_i, $C_D(v_i)$, is simply the number of edges that traverse the vertex. It can be interpreted as the amount of information received by a vertex (in-degree) or the amount of information disseminating from a vertex through the graph (out-degree).

$$C_D(v) = \deg(v) \quad (4)$$

The betweenness of a vertexv_i, $C_B(v_i)$, is defined as the fraction of geodesic distances between all pairs of vertices which traverse the vertex of interest.

$$C_B(v_i) = \sum_{j,k} \frac{d_{jk}(v_i)}{d_{jk}} \quad (5)$$

where d_{jk} is the geodesic distance between v_j and v_k while $d_{jk}(v_i)$ is the geodesic distance between v_j and v_k which passes through the vertex v_i. As can be seen from Equation 5, a vertex

with a high betweenness lies along a large fraction of geodesic distances within the graph so that its removal from the graph could cause a large disconnection.

Closeness of a vertex v_i, $C_C(v_i)$, measures how many steps are needed to reach every other vertices of the graph fromv_i.

$$C_C(v_i) = \sum_j \frac{1}{d(v_i,v_j)} \quad (6)$$

3.2.Graph metrics

Based on the aforementioned vertex centrality measures, a set of corresponding centrality measures can be defined for a graph. In this regard, 'degree', 'betweenness', and 'closeness centrality' metrics of a graph can be calculated using Equation 7:

$$C(G) = \sum_{i=1}^{|V|} C(v^*) - C(v_i) \quad (7)$$

where $C(G)$ is the graph-level centrality measure; $C(v_i)$ is the vertex-level centrality measure; v^* is a vertex of the graph for which the centrality measure of interest is maximum. It is worth noting that $C(v_i)$ and $C(v^*)$ are calculated from Equations 4-6.

The density q of a graph is the ratio of the number of edges m to the maximum number of possible edges $\frac{n(n-1)}{2}$ which occur in a complete graph with n vertices [32]. It is usually used as measure of linkedness or sparseness of a graph [22]:

$$q = \frac{2m}{n(n-1)} \quad (8)$$

Average node degree $k = \frac{2m}{n}$ is a basic measure of the graph connectivity compared to a lattice-like graph [22].

4. Application of Bayesian network to domino effect modeling

4.1.Bayesian network

Bayesian network (BN) is a directed acyclic graph (DAG) for reasoning under uncertainty [33], with a wide variety of applications in risk, safety, and reliability analysis of dependent and complex systems [34]. BN takes advantage of a flexible graphical structure to represent the (causal) relationships between the components of a system using vertices and edges. The type and strength of these relationships are defined using conditional probability tables. BN uniquely

factorizes the joint probability distribution of a set of random variables $X = \{X_1, X_2, \dots, X_n\}$ using the chain rule and d-separation criteria as the product of the probabilities of each variable conditioned on its immediate parents (its direct causes):

$$P(X_1, X_2, \dots, X_n) = \prod_{i=1}^{n} P(X_i|\pi(X_i)) \quad (9)$$

where $\pi(X_i)$ is the parent set of X_i. BN uses Bayes' theorem to conduct belief updating given new evidence E:

$$P(X|E) = \frac{P(X,E)}{P(E)} = \frac{P(X,E)}{\sum_X P(X,E)} \quad (10)$$

More detailed information on BN can be found in [35,36].

4.2.Cascading effect modeling

In this work we apply a methodology introduced in [20] to model cascading effects using BN. Since the modeling procedure has been explained in detail elsewhere [20], we only recapitulate the main steps for the sake of brevity.

1. Credible units of the process plant are identified based on their hazardous material inventory, and presented as the vertices (nodes) of the BN.
2. After the primary unit was identified, possible accident scenarios are determined considering the types of the unit and chemical inventory as well as the physical and operational conditions.
3. The magnitude of the escalation vectors generated by each accident scenario is quantified at neighboring units (target units).
4. The target units at which the magnitude of escalation vectors are greater than corresponding threshold values [25] are identified as secondary units affected by the primary accident.
5. Edges are drawn from the primary unit to the secondary units. The conditional probabilities of the secondary units being damaged by the primary unit can be estimated using probit models (see e.g., Table 1 and Equation 2).
6. Steps 2 to 5 are repeated for the secondary units to identify tertiary units and so forth.

For the sake of clarification, the conditional probability table of X4 in the BN of Figure 1 has been calculated using probit models in Table 1 [9] and Equation 2 (or 3), and presented in Table 2. It should be noted that the conditional probability of X4 not being affected during the

cascading effect, i.e., $P(X4 = Safe|X1, X2, X3)$, can be readily obtained from Table 2 as $P(X4 = Safe|X1, X2, X3) = 1 - P(X4 = Fire|X1, X2, X3)$.

Table 2. Conditional probability of X4 in the BN of Figure 1.

X1	X2	X3	X4 = Fire
Fire	Fire	Fire	8.30E-05
Fire	Fire	Safe	1.38E-06
Fire	Safe	Fire	1.38E-06
Fire	Safe	Safe	0
Safe	Fire	Fire	3.94E-06
Safe	Fire	Safe	0
Safe	Safe	Fire	0
Safe	Safe	Safe	0

5. Vulnerability analysis

5.1.Unit vulnerability analysis

In this work, we demonstrate the application of graph metrics to vulnerability analysis of process plants through a number of hypothetic fuel storage plants. To examine the applicability of vertex metrics in identifying critical units within a process plant, consider a fuel storage plant including eight identical atmospheric storage tanks containing benzene (C_6H_6) as depicted in Figure 2.

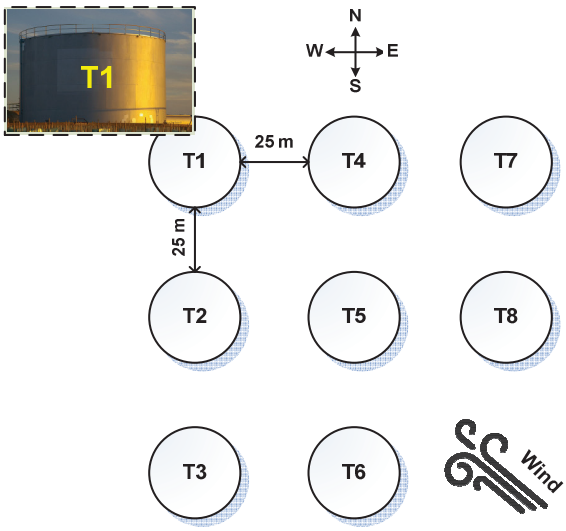

Figure 2. Schematic of a storage plant consisting of eight atmospheric storage tanks of benzene. The wind is gusting with a speed of 5 m/s from South East.

For illustrative purposes, pool fire and heat radiation have been considered the only accident scenario and escalation vector, respectively, for the storage tanks. Considering equal type (atmospheric storage tank) and size ($200\ m^3$) for all the tanks, the same chemical contained (benzene), and apparently identical operational and environmental conditions, it would not be straightforward to identify the most critical initiating unit which could be used as the primary unit in the cascading effect modeling. In order to present the storage plant of Figure 2 as a graph with eight vertices, the edges of the graph need to be specified. In the context of cascading effect modeling, the escalation vectors (heat radiation in this study) form the edges of the graph. To calculate the intensity of escalation vectors, we use the freely accessible software ALOHA (Areal Locations of Hazardous Atmospheres) [37]. ALOHA [37] takes advantage of commonly-used mathematical models such as Gaussian model and heavy gas dispersion model to present an accident scenario consequences under a variety of meteorological conditions (e.g., wind speed and direction, atmospheric stability class, air temperature and humidity), equipment specifications (e.g., equipment geometry, layout, and leakage diameter), and chemical substance characteristics (e.g., temperature, burning ratio, density, etc.).

Assuming a wind speed of $5\ m/s$ measured at $10\ m$ above the ground and gusting from the South East, air temperature of $15^o\ C$, relative humidity of 50%, a partly cloudy sky, and stability class of B, and a circular opening diameter of $15\ cm$ for leakage, the heat radiation intensity received by T_j from T_i, denoted by Q_{ij}, are calculated by ALOHA [37] as tabulated in Table 3.

Table 3. Heat radiation intensities (kW/m^2) received by T_j from T_i

	T_j							
T_i	T1	T2	T3	T4	T5	T6	T7	T8
T1	0	9.58	2.94	9.58	4.53	2.11	2.94	2.11
T2	24.8	0	9.58	8	9.58	4.53	2.85	2.94
T3	5.57	24.8	0	3.67	8	9.58	2	2.85
T4	24.8	8	2.85	0	9.58	2.94	9.58	4.53
T5	16	24.8	8	24.8	0	9.58	8	9.58
T6	4.76	16	24.8	5.57	24.8	0	3.67	8
T7	5.57	3.67	2	24.8	8	2.85	0	9.58
T8	4.76	5.57	3.67	16	24.8	8	24.8	0

Assuming $Q_{th} = 15\ kW/m^2$ as the threshold value [25], the credible heat radiation intensities which are greater than the threshold value have been represented by solid edges in the graph of Figure 3.

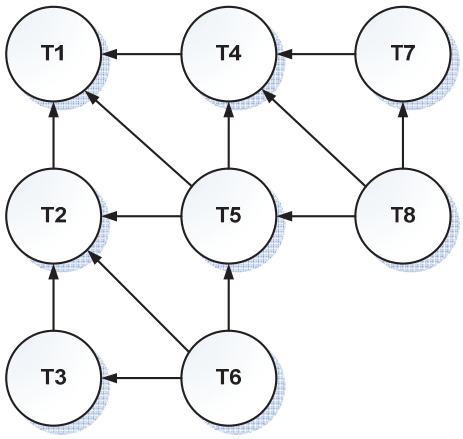

Figure 3. Graph consisting of storage tanks as vertices and escalation vectors (heat radiation) as edges. An edge represents a heat radiation intensity greater than threshold value (Q_{th} = 15 kW/m^2).

To quantify the vertex metrics, we implemented the graph of Figure 3 in an open-source graph manipulation software igraph [38] which can be used as a dynamic library in the freely available statistical software R [39]. The centrality metrics for the vertices of the graph of Figure 3 have been calculated using igraph [38] and listed in Table 4.

Table 4. Vertex metrics for the graph shown in Figure 3.

Vertex	Degree	Closeness	Betweenness
T1	0	0.0179	0.00
T2	1	0.0207	**2.13**
T3	1	0.0245	0.533
T4	1	0.0207	**2.13**
T5	**3**	**0.0303**	**3.87**
T6	**3**	**0.0548**	0.00
T7	1	0.0245	0.533
T8	**3**	**0.0548**	0.00

As can be noted from Table 4, the tanks T5, T6, and T8 have the largest degree and closeness centrality scores while T5, T4, and T2 have the largest betweenness scores. Thus, to identify the most critical initiating unit, individual BNs have been developed for T2, T4, T5, and T6 as primary units in Figure 4. It is worth noting that since escalation vectors with magnitudes lower than 15 kW/m^2 are still likely to cause damage through synergistic effect [20], in this study the heat radiation intensities with magnitudes between 8 and 15 kW/m^2 have also been included in the BN model to account for possible synergistic effects. These heat radiations have been distinguished by dashed edges in Figure 4, implying they are not able to cause credible damage individually but together. Further, since the centrality scores of T8 were exactly the same as of T6, the BN of T8 has not been displayed in Figure 4. In the BNs of Figure 4, primary, secondary, tertiary, and quaternary units have been highlighted gray, yellow, orange, and red, respectively. Further, those units that have been untouched during the cascading effect have been left uncolored.

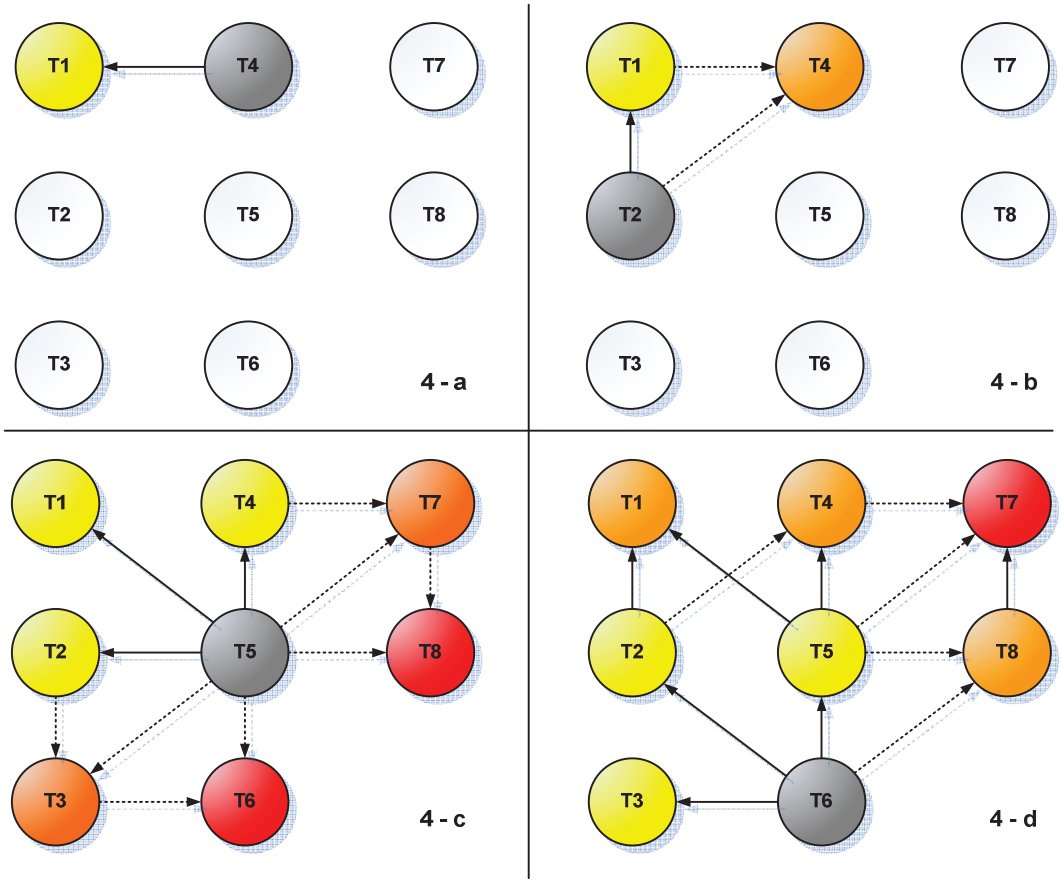

Figure 4. Bayesian networks for cascading effects starting from T4 (4-a), T2 (4-b), T5 (4-c), and T6 (4-d) as the primary units. Primary, secondary, tertiary, and quaternary units are highlighted gray, yellow, orange, and red, respectively. Units which are remained unaffected during cascading effect are left uncolored. Solid edges represent heat radiations greater than 15 kW/m^2 while dashed edges refer to heat radiations between 8 and 15 kW/m^2.

As can be noted from Figure 4, T2 (4-b) and T4 (4-a) would not result in wide-spread cascading effects throughout the process plant. Hence, only BNs of T5 (4-c) and T6 (4-d) were considered and analyzed quantitatively to determine which unit would lead to a more severe cascading effect if selected as the primary unit. The BNs were modeled in the freely available software GeNIe [40], and the results were presented in Table 5. It is worth noting that the prior probability of pool fire in primary units has been considered as 1E-05 [20]. Furthermore, conditional probabilities needed in BN modeling have been calculated by plugging the heat radiation

intensities given in Table 3 into the probit function given in Table 1 for atmospheric storage tanks; then, the resulted probit values have been converted to probabilities using Equation 2 or 3.

In order to compare the severity of cascading effects, their probabilities at consecutive levels have also been calculated using the BN methodology as shown in Table 5. For instance, according to the BN in which T6 is the primary unit (Figure 4-d), the probabilities of the first level D1 and second level D2 of the cascading effect is $P(D1) = P(T2 \cup T3 \cup T5)$ and $P(D2) = P(T1 \cup T4 \cup T8)$, respectively. It should be noted these probabilities can readily be quantified by adding vertices D1 and D2 to the respective BNs and connecting them to the corresponding nodes by means of OR-gate conditional probability tables [20]. As can be seen from Table 5, aside from identical probabilities of D1 for the all the units as the primary unit, T6 (or T8) results in larger probabilities for D2 and D3 compared to T5.

Table 5. Updated probabilities of events given a pool fire in primary event.

	Primary unit		
Vertex	T5	T6	T8
T1	4.03E-07	2.36E-11	2.36E-11
T2	2.92E-05	4.03E-07	8.53E-10
T3	2.92E-11	2.92E-05	1.02E-14
T4	2.92E-05	8.53E-10	4.03E-07
T5	**1.00E+00**	2.92E-05	2.92E-05
T6	6.95E-17	**1.00E+00**	3.15E-11
T7	2.92E-11	1.02E-14	2.92E-05
T8	6.95E-17	3.15E-11	**1.00E+00**
D1	5.88E-05	5.88E-05	5.88E-05
D2	6.10E-11	9.08E-10	9.08E-10
D3	1.03E-16	1.02E-14	1.02E-14

Comparing the probability of cascading effects originated from the primary units T5, T6, and T8 (Table 5) with the vertex metrics of the same units (Table 4), it can be implied that the primary unit (initiating unit) with the largest closeness score would result in the highest probabilities for cascading effects. This implication is in compliance with both the propagation mechanism of cascading effects and the physical interpretation of the closeness metric. That is, since a unit with a larger closeness score can reach to a larger number of other units (see the definition of closeness in Section 3.1), we can expect this unit to affect more number of units within a

cascading effect. Thus, in order to prevent or reduce the probability of catastrophic cascading effects in process plants, units can be rank-ordered based on their closeness scores so that preventive measures can be allocated to the most critical primary units.

Considering the vertex metrics in Table 4, more information about criticality of units can be elicited. Figures 5-a and 5-b depict the BNs developed for modeling cascading effects triggered by T6 and T8 as the most critical initiating units (with largest closeness scores), respectively. It should be noted that Figure 5-a is the same as Figure 4-d and has been repeated here for the sake of further comparison. Figures 5-c and 5-d depict the same BNs in 5-a and 5-b, respectively, yet with the only difference that the nodes with largest betweenness scores, i.e., T5, T4, and T2, have been isolated (e.g., fireproofed) so that they cannot be entailed in the cascading effects triggered by T6 or T8. These isolated units have been indicated in Figures 5-c and 5-d as double-outlined nodes implying their higher resistance against heat radiations emitted from T6 or T8.

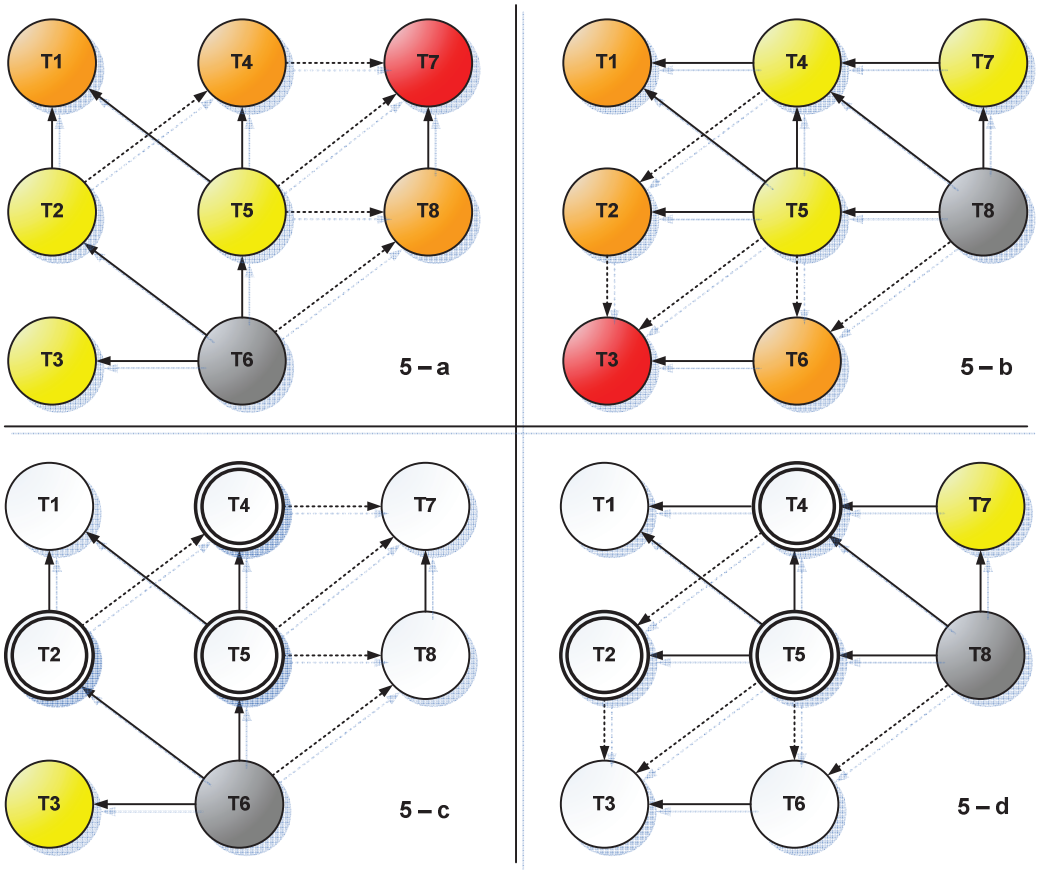

Figure 5. BNs of cascading effects triggered by T6 (5-a and 5-c) and T8 (5-b and 5-d). Figures 5-c and 5-d display cases where units with high betweenness scores, i.e., T5, T4, and T4, are not contributing to the cascading effects. These units have been indicated as double-outlined nodes.

As evidenced in Figure 5, having nodes with high betweenness protected by isolating them, significantly limits the propagation of a cascading effect through the process plant. Since betweenness is a metric to measure how much a node contributes to geodesic distances within a graph, exclusion of a node with large betweenness from a graph is very likely to disconnect the graph to a large extent. In the context of cascading effect analysis, however, exclusion of a node with high betweenness refers to the isolation of the node by means of fireproofing or other protective measures so that it cannot contribute to a potential cascading effect.

5.2.Plant vulnerability analysis

In this section, we will demonstrate the application of graph-level metrics to measure the plant vulnerability of a process plant in the context of cascading effects. For illustrative purposes, consider two common arrangements of chemical storage plants in Figure 6, which are rectangle (Figure 6-a) and triangle (Figure 6-b) layouts [41]. It has been further assumed that the tanks are of the same type and size as described in the storage plant of Figure 2 with the same environmental and operational conditions previously defined for ALOHA [37].

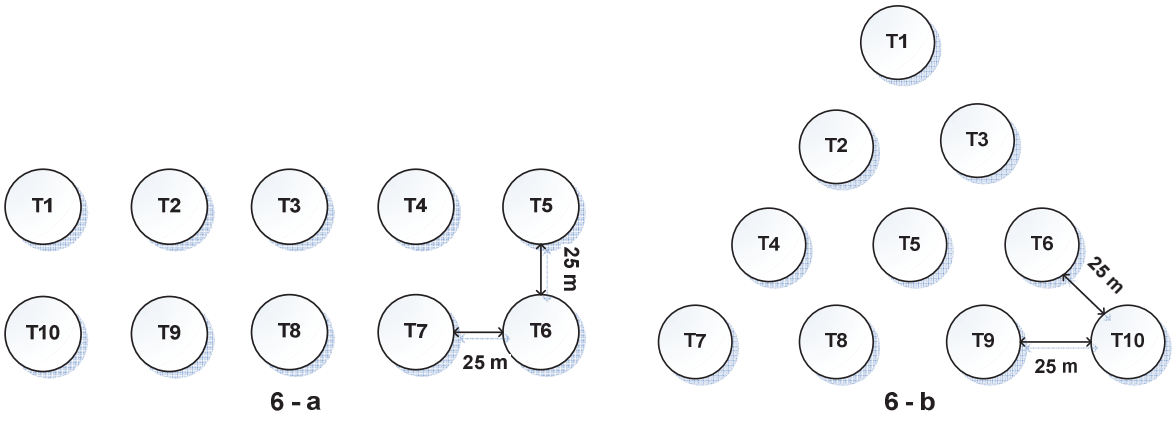

Figure 6. Common layouts for chemical storage plants.

Heat radiation intensities were calculated for all pairs of units by ALOHA [37], and the resulting graphs were implemented in igraph [38] to quantify graph-level metrics. Table 6 presents the graph centrality measures, graph density q and average degree k. As can be seen from Table 6,

all the graph-level metrics of the triangle layout are less than those of the rectangle layout except the closeness centrality measure. Thus, to find out which layout would result in a higher probability for potential cascading effects, we model cascading effects within both layouts using BN. To model the potentially most devastating cascading effect in each layout, the vertex closeness metrics for the both graphs have been quantified as listed in Table 7 (columns 2 and 5) so that the most critical initiating (primary) unit in each graph could be identified. Consequently, T6 and T10 are identified as the most critical primary units in the rectangle (Figure 7-a) and triangle (Figure 7-b) layouts, respectively. The probabilities of pool fires in the other tanks as well as the probabilities of consecutive levels of cascading effects, i.e., D1, D2, D3, and D4, are also presented in Table 7 (columns 4 and 7) given a pool fire in the corresponding primary units.

Table 6. Graph-level metrics for fuel storage plants in Figure 6.

Layout	Degree	Closeness	Betweenness	Density	Avg. degree
Rectangle	0.144	0.311	0.046	0.378	3.4
Triangle	0.089	**0.358**	0.041	0.267	2.4

Table 7. Vertex-level metrics and probabilities for fuel storage plants in Figure 6.

	Rectanglelayout			Triangle layout		
Vertex	Closeness	Betweenness	Posterior Probability¥	Closeness	Betweenness	Posterior Probability€
T1	0.100	0.00	4.95E-20	0.100	0.00	2.98E-11
T2	0.111	4.17	1.19E-15	0.100	0.00	9.10E-12
T3	0.123	**5.50**	2.52E-11	0.125	2.83	9.61E-08
T4	0.136	3.83	4.03E-07	0.100	0.00	9.18E-13
T5	0.150	0.00	3.13E-05	0.125	**4.33**	1.95E-08
T6	**0.429**	0.00	**1.00E+00**	0.188	**3.50**	3.00E-04
T7	0.273	**5.17**	3.13E-05	0.100	0.00	3.07E-14
T8	0.191	**6.50**	9.80E-10	0.125	2.83	9.80E-10
T9	0.143	4.83	3.07E-14	0.188	**3.50**	3.13E-05
T10	0.111	0.00	9.60E-19	0.450	0.00	**1.00E+00**
D1			6.30E-05			3.00E-04
D2			1.00E-09			1.17E-07
D3			3.19E-14			3.98E-11
D4			1.01E-18			N/A

¥Posterior probabilities given a pool fire in T6 as the primary unit in the rectangle layout.

€ Posterior probabilities given a pool fire in T10 as the primary unit in the triangle layout.

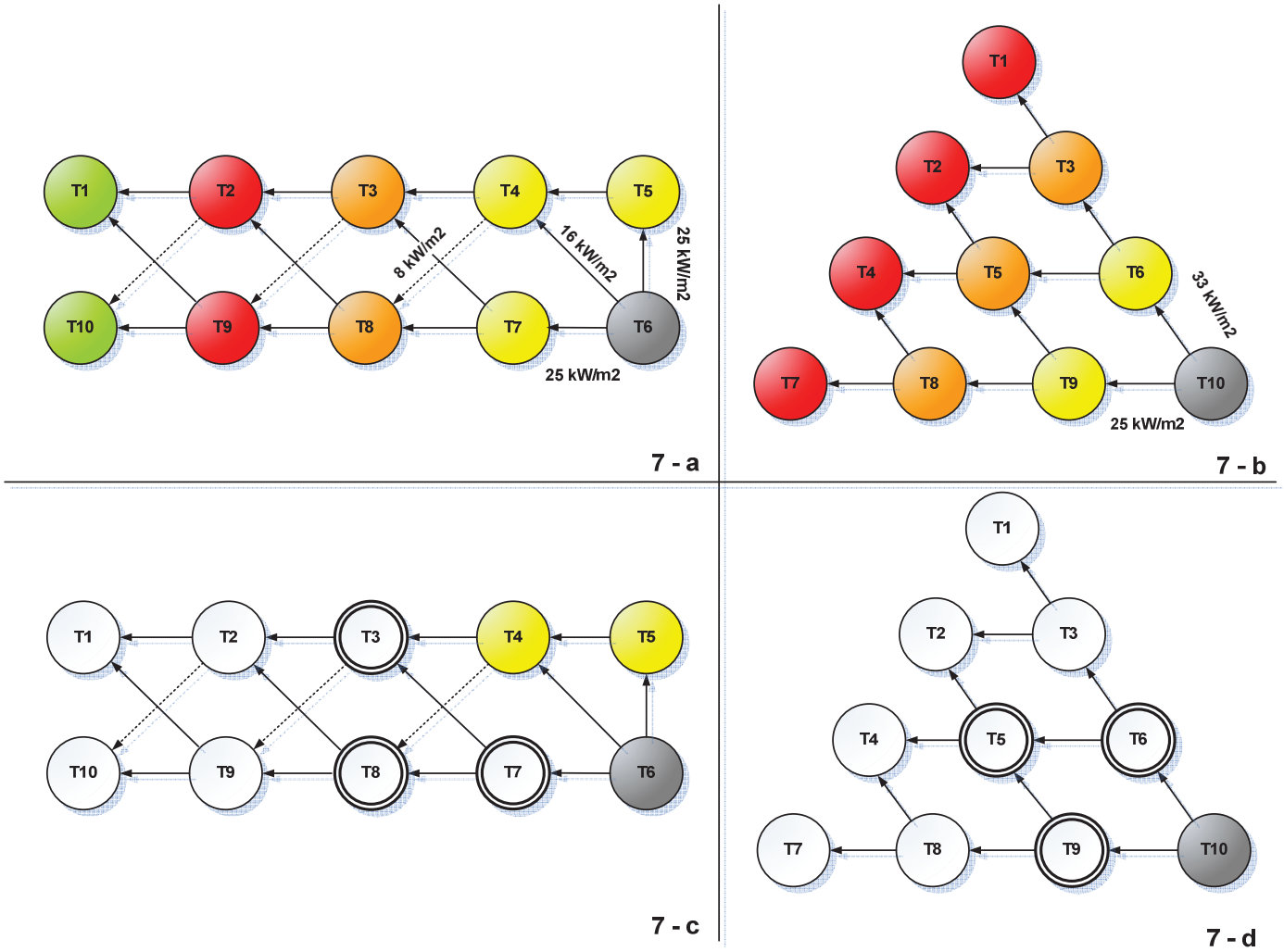

Figure 7. Cascading effects in the rectangle and triangle storage plant layouts. Figures (7-a) and (7-b) illustrate the BNs to model the propagation of cascading effects where the primary, secondary, tertiary, and quaternary units have been highlighted grey, yellow, orange, red, and green, respectively. Figures (7-c) and (7-d) display the isolated units as double-outlined nodes.

As can be noted from the probabilities of D1, D2, D3, and D4 in Table 7, the triangle layout could result in higher probabilities for the respective cascading effects. Considering the graph-level metrics in Table 6, it can consequently be inferred that the graph with larger graph-level closeness score is more vulnerable to cascading effects. Having the graphs (BNs) in Figures 7-a and 7-b, the vertex-level betweenness scores have also been presented in Table 7 (columns 3 and 6). Figures 7-c and 7-d display the same graphs in which the nodes with largest betweenness scores have been double-outlined, implying their isolation can significantly limit the propagation of a potential cascading effect within the process plant.

5.3.Discussion

In the previous sections, we demonstrated that certain graph theory metrics can effectively be used as a quick and reliable tool in the vulnerable analysis of process plants. Although BN has proved to be a versatile methodology for both risk analysis [20] and vulnerability analysis of chemical plants (this study), the application of such graph metrics as a complementary tool could increase the efficacy of modeling and significantly reduce the time of analysis. For example, regarding the application of BN to unit vulnerability analysis, in the absence of vertex-level closeness metric to identify the most critical primary unit, individual BNs should be developed for each unit of the process plant as the primary unit to determine which unit would result in a more severe cascading effect. The analysis would become even more cumbersome and time-consuming in the case of plant vulnerability analysis where the above-mentioned individual BNs should be developed and analyzed for each process plant layout separately.

However, it should be noted that the identification of critical units and layouts using graph theory metrics in this study has been under the influence of a variety of topological, meteorological, and operational factors the change of which could result in a different set of critical units and layouts. For example, consider the process plant of Figure 2 with a wind direction from north instead of south-east. Figure 8-a depicts a graph representation of the process plant, where the arcs represent the heat radiation intensities greater than the threshold value $Q_{th} = 15\ kW/m^2$. Having the graph of Figure 8-a implemented in igraph [38], the vertex-level closeness and betweenness scores have been calculated and listed in Table 8. As can be seen from the table, the unit T4 has the largest closeness score while T1, T2, and T5 have the largest betweenness scores. Considering T4 as the primary unit, the corresponding BN for modeling the potential cascading effect has been developed in Figure 8-b, in which heat radiation intensities lower than the threshold value have been also included to account for possible synergistic effects (dashed arcs). Figure 8-c depicts the same BN in which T1, T2, and T5 have also been isolated from the cascading effect, indicated as double-outlined nodes. As evident from this example, with a change in wind direction, a different set of critical units have been identified using the graph metrics. As a result, it is advised that the parameters used in ALOHA [37] to calculate the escalation vectors (e.g., wind speed and direction) represent the predominant characteristics of the process plant under consideration.

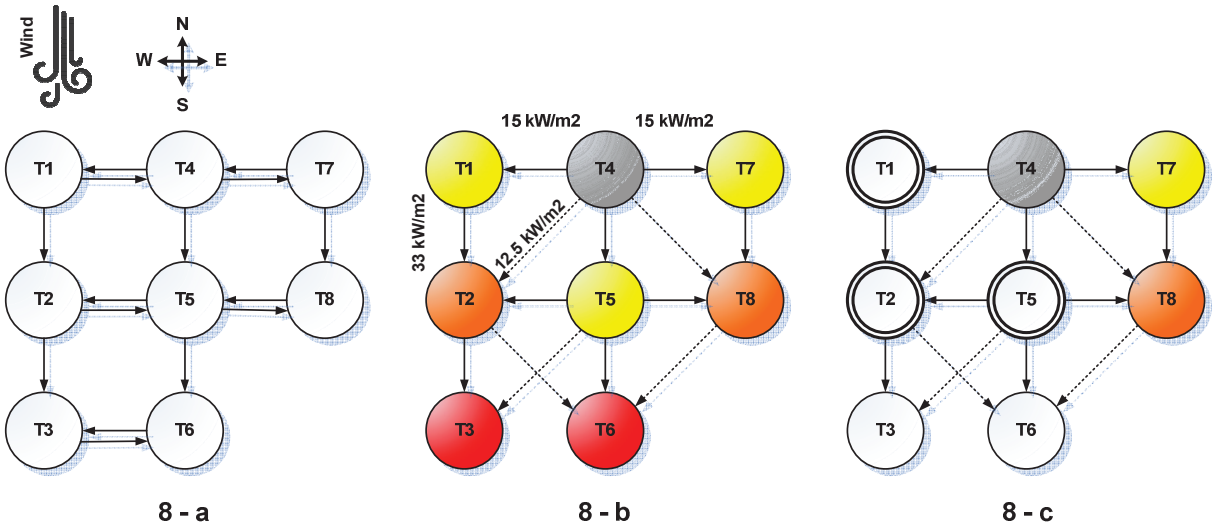

Figure 8. Identification of critical units in the process plant of Figure 2 where the wind gusts from the North to South. Figure 8-a depicts the heat radiations intensities greater than the threshold value Q_{th} = 15 kW/m^2. Figure 8-b displays the corresponding BN with T4 as the primary unit. Figures 8-c shows the same process plant where units with high betweenness scores, i.e., T1, T2, and T5, have been isolated.

Table 8. Vertex metrics for the graph shown in Figure 8-a.

Vertex	Closeness	Betweenness
T1	0.1905	**1.00**
T2	0.0377	**3.00**
T3	0.0206	0.00
T4	**0.2350**	0.00
T5	0.0385	**2.50**
T6	0.0206	0.00
T7	0.1600	0.50
T8	0.0363	0.00

In the present study we showed that certain graph metrics such as closeness and betweenness scores can effectively be used for both unit and plant vulnerability analysis while considering the heat radiation as the only escalation vector in cascading effects. However, to establish these graph metrics as a reliable tool in the identification of critical units and layouts in process plants a broader range of process units (e.g., pressurized equipment), accident scenarios (e.g.,

explosions), and escalation vectors (e.g., overpressure) should be taken into account in future work.

6. Conclusions

This work has illustrated an application of graph theory to vulnerability analysis of process plants subject to cascading effects. We examined the applicability of a number of graph metrics to both (i) unit and (ii) plant vulnerability analysis of chemical storage plants. In the unit vulnerability analysis, we applied a number of vertex-level metrics such as degree, closeness, and betweenness to identify the most critical primary and intermediate units within a process plant. In the plant vulnerability analysis, however, a set of graph-level metrics such as graph degree, graph closeness, graph betweenness, graph density, and graph average degree were applied to identify the most vulnerable layout which would lead to higher probabilities for a potential cascading effect. The results obtained from graph metrics were compared and verified using a Bayesian network methodology.

We showed that in the unit vulnerability analysis, a primary unit with the largest vertex-level closeness score would result in a higher likelihood and severity for a potential cascading effect compared to its peers in the same process plant. Furthermore, units with relatively larger betweenness values would contribute more than other units to the propagation of a previously started cascading effect. From a plant vulnerability viewpoint, it was demonstrated that for a process plant, a layout (units' arrangement) with relatively larger graph-level closeness score would be more vulnerable to the escalation of cascading effects – in terms of probability and severity – compared to other available layouts for the same process plant.

This study demonstrated that certain graph metrics can effectively be used for a quick and preliminary screening of either vulnerable units or vulnerable layouts in process plants. These vulnerable units and layouts can further be investigated in more detail using available methods such as Bayesian Network analysis.

References

[1] Reniers G, Cozzani V. Domino Effects in the Process Industries: Modeling, Prevention and Managing. Elsevier, 2013.

[2] Darbra RM, Palacios A, Casal J. Domino effect in chemical accidents: Main features and accident sequences. Journal of Hazardous Materials, 2010; 183: 565–573.

[3] The guardian (2010). http://www.theguardian.com/uk/2010/jun/18/buncefield-fire-oil-company-guilty. Last accessed on November 12, 2014.

[4] Bagster DF, Pitblado RM. The estimation of domino incident frequencies – An approach. Process Safety and Environmental Protection, 1991; 69: 195–199.

[5] Delvosalle C, Domino effects phenomena: definition overview and classification, in: Proceedings of the European Seminar on Domino Effects, Leuven, Belgium, 1996.

[6] Gledhill J, Lines I. Development of Methods to Assess the Significance of Domino Effects from Major Hazard Sites. CR Report 183, Sudbury, UK: Health and Safety Executive, 1998.

[7] Khan F, Abbasi SA. Models for domino analysis in chemical process industries. Process Safety Progress, 1998; 17: 107–123.

[8] Cozzani V, Salzano E. The quantitative assessment of domino effects caused by overpressure part I. probit models. Journal of Hazardous Materials, 2004; A107: 67–80.

[9] Cozzani V, Gubinelli G, Antonioni G, Spadoni G, Zanelli S. The assessment of risk caused by domino effect in quantitative area risk analysis. Journal of Hazardous Materials, 2005; A127: 14–30.

[10] Cozzani V, Gubinelli G, Salzano E. Escalation thresholds in the assessment of domino accidental events. Journal of Hazardous Materials, 2006; 129: 1–21.

[11] Reniers G, Dullaert W, Ale B, Soudan K. The use of current risk analysis tools evaluated towards preventing external domino accidents. Journal of Loss Prevention in Process Industries, 2005; 18: 119–126.

[12] Reniers G, Dullaert W. DomPrevPlanning: User-friendly software for planning domino effects prevention. Safety Science, 2007; 45: 1060–1081.

[13] Reniers G, Dullaert W. Knock-on accident prevention in a chemical cluster. Expert Systems with Applications, 2008; 34(1): 42-49.

[14] Reniers G, Dullaert W, Soudan K. Domino effects within a chemical cluster: A game-theoretical modeling approach by using Nash-equilibrium. Journal of Hazardous Materials, 2009; 167: 289–293.

[15] Reniers G. An external domino effects investment approach to improve cross-plant safety within chemical clusters. Journal of Hazardous Materials, 2010; 177(1-3): 167-174.

[16] Reniers G, Audenaert A. Preparing for major terrorist attacks against chemical clusters: Intelligently planning protection measures w.r.t. domino effects. Process Safety and Environmental Protection, 2014; 92(6): 583-589.

[17] Landucci G, Gubinelli G, Antonioni G, Cozzani V. The assessment of the damage probability of storage tanks in domino events. Accident analysis and Prevention, 2009; 41: 1206–1215.

[18] Nguyen QB, Mebarki A, Ami Saada R, Reimeringer M. Integrated probabilistic framework for domino effect and risk analysis. Journal of Advances in Engineering Software, 2009; 40: 892–901.

[19] Abdolhamidzadeh B, Abbasi T, Rashtchian D, Abbasi SA.A new method for assessing domino effect in chemical process industry. Journal of Hazardous Materials, 2010; 182: 416–426.

[20] Khakzad N, Khan F, Amyotte P, Cozzani V. Domino effect analysis using Bayesian networks. Risk Analysis, 2013; 33(2): 292–306.

[21] Khakzad N, Khan F, Amyotte P, Cozzani V. Risk management of domino effects considering dynamic consequence analysis. Risk Analysis, 2014; 34(6): 1128–1138.

[22] Yazdani A, Appiah Otoo R, Jeffery P. Resilience enhancing expansion strategies for water distribution systems: A network theory approach. Environmental Modelling & Software, 2011; 26: 1574-1582.

[23] Johansson J, Hassel H, Zio E. Reliability and vulnerability analyses of critical infrastructures: Comparing two approaches in the context of power systems. Reliability Engineering and System Safety, 2013; 120: 27-38.

[24] Johansson J, Hassel H. An approach for modeling interdependent infrastructures in the context of vulnerability analysis. Reliability Engineering and System Safety, 2010; 95: 1335-1344.

[25] Cozzani V, Tugnoli A, Slazano E. The development of an inherent safety approach to the prevention of domino effects. Accident Analysis and Prevention 2009; 41: 1216-1227.

[26] Cozzani V, Tugnoli A, Salzano E. Prevention of domino effect: From active and passive strategies to inherently safer design. Journal of Hazardous Materials, 2007; A139: 209–219.

[27] Reniers G, Sorensen K, Khan F, Amyotte P. Resilience of chemical industrial areas through attenuation-based security. Reliability Engineering and System Safety 2014; 131: 94-101.

[28] Van Den Bosh CJH, Weterings RAMP. Methods for the Calculation of Physical Effects (Yellow Book).The Hague, NL: Committee for the Prevention of Disasters, 1997.

[29] CCPS. Guidelines for Chemical Process Quantitative Risk Analysis, 2nd edition. New York: AIChE, 2000.

[30] Assael MJ, Kakosimos KE. Fires, Explosions, and Toxic Gas Dispersions: Effects Calculation and Risk Analysis. NW: CRC Press, Taylor and Francis Group, 2010.

[31] Freeman LC. Centrality in social networks I: conceptual clarification, Social Network 1 (1979) 215–239.

[32] Wasserman S, Faust K. (1994). Social Network Analysis: Methods and Applications. Cambridge: Cambridge University Press.

[33] Pearl J. 1988. Probabilistic Reasoning in Intelligent Systems. San Francisco, CA: Morgan Kaufmann.

[34] Khakzad N, Khan F, Amyotte P. Safety analysis in process facilities: Comparison of fault tree and Bayesian network approaches. Reliability Engineering and System Safety, 2011; 96: 925-932.

[35] Neapolitan R. 2003. Learning Bayesian Networks. Prentice Hall, Inc. Upper Saddle River, NJ, USA.

[36] Jensen FV, Nielsen TD. 2007. Bayesian Networks and Decision Graphs, 2nd edition. New York: Springer.
[37] ALOHA. US Environmental Protection Agency, National Oceanic and Atmospheric Administration. Available online at: http://www.epa.gov/OEM/cameo/aloha.htm.
[38] Csardi G, Nepusz T. 2006. The igraph software package for complex network research. InterJournal; Complex Systems, 1695.

[39] R Development Core Team, 2009. R: A Language and Environment for Statistical Computing, R Foundation for Statistical Computing, Vienna, Austria. Available online at http://www.R-project.org.

[40] GeNie. Decision Systems Laboratory, University of Pittsburg. Available online at: http://www.genie.sis.pitt.edu.
[41] Sengupta A, Gupta AK, Mishra IM. Engineering layout of fuel tanks in a tank farm. Journal of Loss Prevention in the Process Industries, 2011; 24:568–574.